

PAPER • OPEN ACCESS

On the formation of antihydrogen beams using travelling optical lattices

To cite this article: N Madsen and M Charlton 2021 *New J. Phys.* **23** 073003

View the [article online](#) for updates and enhancements.



PAPER

On the formation of antihydrogen beams using travelling optical lattices

OPEN ACCESS

RECEIVED
7 April 2021REVISED
1 June 2021ACCEPTED FOR PUBLICATION
15 June 2021PUBLISHED
30 June 2021Original content from
this work may be used
under the terms of the
[Creative Commons
Attribution 4.0 licence](#).Any further distribution
of this work must
maintain attribution to
the author(s) and the
title of the work, journal
citation and DOI.

N Madsen* and M Charlton*

Department of Physics, Faculty of Science and Engineering, Swansea University, Swansea SA2 8PP, United Kingdom

* Authors to whom any correspondence should be addressed.

E-mail: n.madsen@swansea.ac.uk and m.charlton@swansea.ac.uk

Keywords: antihydrogen, optical lattice, atomic beam, travelling optical lattice

Abstract

The production of beams of antihydrogen atoms using the dipole force provided by a travelling optical lattice to accelerate a sample of the anti-atoms held in a magnetic gradient atom trap is investigated. By considering current and near-future antihydrogen trapping capabilities we find that useful fluxes of the anti-atoms can be achieved with directional properties that can be manipulated using laser parameters such as pulse duration and frequency chirp rate. Applications of the beams are briefly discussed.

1. Introduction

Recent years have seen great progress in research with antihydrogen, $\bar{\text{H}}$, the antiproton (\bar{p})–positron (e^+) bound state. It is now possible to routinely capture anti-atoms in magnetic minimum traps [1–3], hold onto them for extended periods if required [4], and accumulate them over several formation cycles [5]. These advances have allowed the first experiments to be performed on antihydrogen [6–8] including: observations of ground state hyperfine [9] and the 1S–2S transitions [10], and the observation of excited state fine structure [11]; measurements of the spectrum of the ground state hyperfine levels [12] and the 1S–2S lineshape [13]; observation of the anti-atom Lyman- α (1S–2P) transition [14] and its application to laser-cool the anti-atom [15]. Furthermore, progress in making directed fluxes of the anti-atom has been reported [16, 17] (and see below), whilst others are developing analogous capabilities [18–20] exploiting charge exchange in \bar{p} –Ps (positronium, the electron–positron bound state) interactions [21, 22].

To date, most $\bar{\text{H}}$ formation experiments have exploited \bar{p} – e^+ interactions, and at typical conditions of positron density and temperature the three-body reaction



is dominant (e.g., [23–25]). It has been well-documented [26–32] that this process produces very weakly bound states that are susceptible to break up due to further collisions in the e^+ plasma, and as result of ambient electric fields. In addition, the multitude of \bar{p} interactions with positrons leads to their rapid radial diffusion [31], and the emission of $\bar{\text{H}}$ over a wide angular range [33, 34]. Both of these factors may mean that reaction 1 is not ideal for experiments requiring beams of ground state $\bar{\text{H}}$ atoms.

A typical $\bar{\text{H}}$ experiment uses so-called Penning–Malmberg traps to hold and manipulate the \bar{p} and e^+ clouds prior to mixing. Such traps employ a combination of electric and magnetic fields, with the latter typically in the tesla range to ensure efficient \bar{p} capture and cooling [35] from the CERN Antiproton Decelerator (AD) [36], and to aid in the capture and manipulation of electron and positron clouds. Such fields can, for instance, influence the outcomes of reaction 1 and will perturb the antihydrogen properties, such as transition frequencies, via the Zeeman and Stark effects. Furthermore, the magnetic gradient forces required for the operation of $\bar{\text{H}}$ traps are not negligible when compared to the size of the gravitational force on the anti-atom, and complicate gravity studies using trapped $\bar{\text{H}}$ samples [37]. Consequently, the formation and application of $\bar{\text{H}}$ beams has been considered such that the anti-atoms can be transported to a field-free region.

Most of the experiments envisaged to explore antihydrogen spectroscopy require $\bar{\text{H}}$ in its ground state, irrespective of whether the investigation is conducted in beam-like or trap-like environments. In the latter, the long confinement times [3–5] ensure that the sample is (positron) spin-polarised and that the ground state is reached (actually within about 1 s, irrespective of the initial state upon formation), and this has facilitated some of the recent advances [9–15]. However, in beam-like scenarios, whereby the $\bar{\text{H}}$ propagates directly after formation via reaction 1, there is no guarantee that there is a substantial ground state, spin-polarised, population (either directly or through in-flight decay from excited states), and the useful flux may be a very small fraction of the overall anti-atom yield, even with the use of beamline focussing. The ASACUSA collaboration first reported the detection of $\bar{\text{H}}$ atoms 2.7 m downstream from their production in a magnetic cusp trap via $e^+ - \bar{p}$ interactions [17]. In that study the measured flux was around 20–30 per hour, constrained by a field ionisation analysis to be in states with a principal quantum number $n \lesssim 29$ from 3×10^5 antiprotons deployed in mixing cycles of 15 min duration. This has been refined in further work [38–40] and most recently by Kolbinger *et al* [41].

An overarching goal for ASACUSA is to pursue an in-beam measurement of the $\bar{\text{H}}$ ground state hyperfine splitting (as a test of CPT symmetry) [42] in a manner similar to a recent experiment on hydrogen [43]. In preparation, the group has also studied, via simulations, the $\bar{\text{H}}$ yield, with emphasis on the production of a low energy beam in a state which can decay to the ground state in-flight [44, 45]. Further work comprised a simulation of the anti-atom trajectories in the ASACUSA cusp trap and proposed hyperfine splitting apparatus, including changes of the magnetic moment, concluding that the experiment required a method to produce antihydrogen in a low excited state, or presumably directly in the ground state [46]. More recent analyses (see for example [47]) have been performed, based upon their hydrogen experiment [43] and upon simulations [48], to estimate the number and speed of $\bar{\text{H}}$ atoms required to reach a relative precision of the frequency of the transition in the region of a part-per-million. In round numbers approximately 8×10^3 ground state $\bar{\text{H}}$ s with a speed of around 10^3 ms^{-1} are needed to interact with microwave radiation in a cavity of length 10 cm. Given the detected downstream yield of $\bar{\text{H}}$ in quantum states low enough to decay to the ground state to enable the hyperfine measurement to be performed, it is thought a substantial (1–2 orders of magnitude) increase in flux will be required [41, 47].

A detailed examination of the formation of $\bar{\text{H}}$ beams from reaction 1 was undertaken recently [34]. These simulations involved full motion of both the positrons and the antiprotons, as is required to derive realistic estimates for the yields and the binding energies of the nascent anti-atoms. In one example a fraction of about 2×10^{-3} of the \bar{p} s injected at a kinetic energy of 0.05 eV along the axis of a 1 cm long positron plasma (at a relatively high density of 10^{15} m^{-3} and a temperature of 15 K) emerge in a single pass through the e^+ s within an angular range of roughly $\pm 6^\circ$. The yield is strongly dependent upon the positron temperature and density, the \bar{p} injection energy and, at densities above about 10^{14} m^{-3} , the radius of injection. The binding energies were found to span a wide distribution in the 10–100s K range [34], and subsequent work has shown that this is also very dependent upon the plasma properties and the injection radius [32].

The present discussion is motivated by the need to consider new ways to produce $\bar{\text{H}}$ beams and has been informed by the recent success of the ALPHA collaboration in accumulating around 10^3 $\bar{\text{H}}$ atoms in a magnetic minimum trap where they have a lifetime against loss of over 60 h [13]. Furthermore, ALPHA's laser excitation of the $1S-2S$ and $1S-2P$ transitions has involved optical access to the $\bar{\text{H}}$ trap, such that it is now feasible to consider a broader scope of $\bar{\text{H}}$ -photon interactions. The current manner of laser access to the $\bar{\text{H}}$ trap is conducive to the introduction of beams overlapping at a small angle, and as a result it is possible to consider optically induced acceleration of the anti-atoms using travelling optical lattices, as has been demonstrated for matter atoms [49, 50]. In section 2 we present a brief summary of the physics of optical lattice acceleration before describing possibilities for its implementation for trapped $\bar{\text{H}}$ in section 3. Further discussion and concluding remarks can be found in section 4.

2. Acceleration of polarisable neutrals using travelling optical lattices

The acceleration process involves the generation of a dipole force using an intense optical field at a frequency far from a resonance of the system under consideration. Such optical forces have been used to transport atoms and molecules, employing high intensity fields to achieve accelerations in the $10^{11}g$ range [51, 52], with the latter increasing by three orders of magnitude if the positronium atom is considered [53]. The dipole force for a far-detuned field is given in the quasi-electrostatic approximation, for a particle with dc polarizability, α , by [54]

$$F = \frac{1}{2}\alpha\nabla E^2, \quad (2)$$

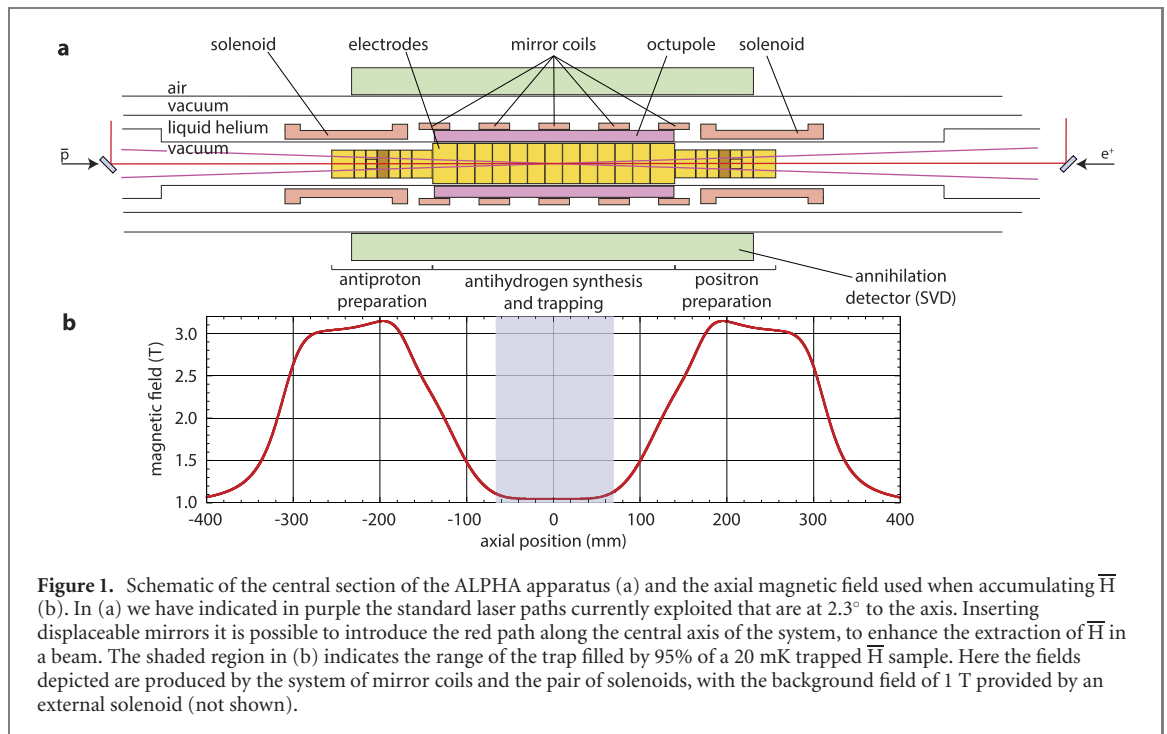


Figure 1. Schematic of the central section of the ALPHA apparatus (a) and the axial magnetic field used when accumulating \bar{H} (b). In (a) we have indicated in purple the standard laser paths currently exploited that are at 2.3° to the axis. Inserting displaceable mirrors it is possible to introduce the red path along the central axis of the system, to enhance the extraction of \bar{H} in a beam. The shaded region in (b) indicates the range of the trap filled by 95% of a 20 mK trapped \bar{H} sample. Here the fields depicted are produced by the system of mirror coils and the pair of solenoids, with the background field of 1 T provided by an external solenoid (not shown).

where E is the optical electric field. The dipole force is proportional to the gradient of the laser intensity, with the latter given by $I = \epsilon_0 c E^2 / 2$, and limited for atomic and molecular species by the onset of multi-photon ionization, which typically occurs at intensities greater than 10^{16} Wm^{-2} or so for the pulse durations considered here (see e.g., [55, 56]). Large intensity gradients can be created by the interference of (near) counter-propagating optical fields, often referred to as an optical lattice. In this type of field the velocity of the lattice, and hence the speed of the particles that are trapped within it, can be controlled by changing the velocity of the optical potential, with the acceleration induced by the field, as implied by equation (2), proportional to the polarizability-to-mass ratio of the particle.

A 1D optical lattice can be formed (in the z -direction) by the interference between two counter-propagating Gaussian beams with optical fields $E_{1,2}(z, r, t)$ which induce a dipole moment in the atom that interacts with the same field to create an optical potential given by $U = -\frac{1}{2} \alpha \langle |E_1(z, r, t) + E_2(z, r, t)|^2 \rangle$. This expression averages over a time that is long compared to the optical period but short compared to the temporal variations in all other quantities. In the case when the magnitude of the wavevectors and the frequencies ($\omega_{1,2}$) of each beam are equal the potential formed is a series of lattice sites separated by approximately one half of the wavelength of the light.

Particles may be trapped within the lattice sites when their energy is less than the well depth, and a detailed treatment can be found elsewhere [49, 57]. If the overlapping fields are at the same frequency at $t = 0$, a group of particles are trapped whose velocity is centred at zero. Acceleration ensues if the frequency difference between the two beams is changed, and a constant acceleration is produced by a linear frequency chirp ($\beta(t) = d(\omega_1 - \omega_2)/dt$) in one of the beams. In the absence of collisions (which is the case for antihydrogen as considered here) the particle motion is independent in r and z such that the relevant force can be computed in isolation. As the gradient along the lattice direction is more than an order of magnitude greater than its radial counterpart, only the z -motion needs to be considered, providing the acceleration is fast compared to the oscillation period in the transverse radial direction [58].

We can make a first estimate of the effect of a 1D travelling lattice on antihydrogen by assuming no radial gradient in the optical field, and by ignoring initial phase shifts between the two beams the relevant equation of motion is

$$\ddot{z} = -a(t) \sin(qz - \beta t^2). \quad (3)$$

The maximum acceleration caused by the lattice is

$$a = \left(\frac{\alpha}{m} \right) \frac{qE_0^2}{2} = \left(\frac{\alpha}{m} \right) \frac{qI_0}{\epsilon_0 c}, \quad (4)$$

where E_0 is amplitude of the beams, with I_0 the attendant maximum laser intensity, and $q = 4\pi/\lambda$ is the lattice wave vector with λ the wavelength of the lasers. For the particle to be trapped and accelerated by the

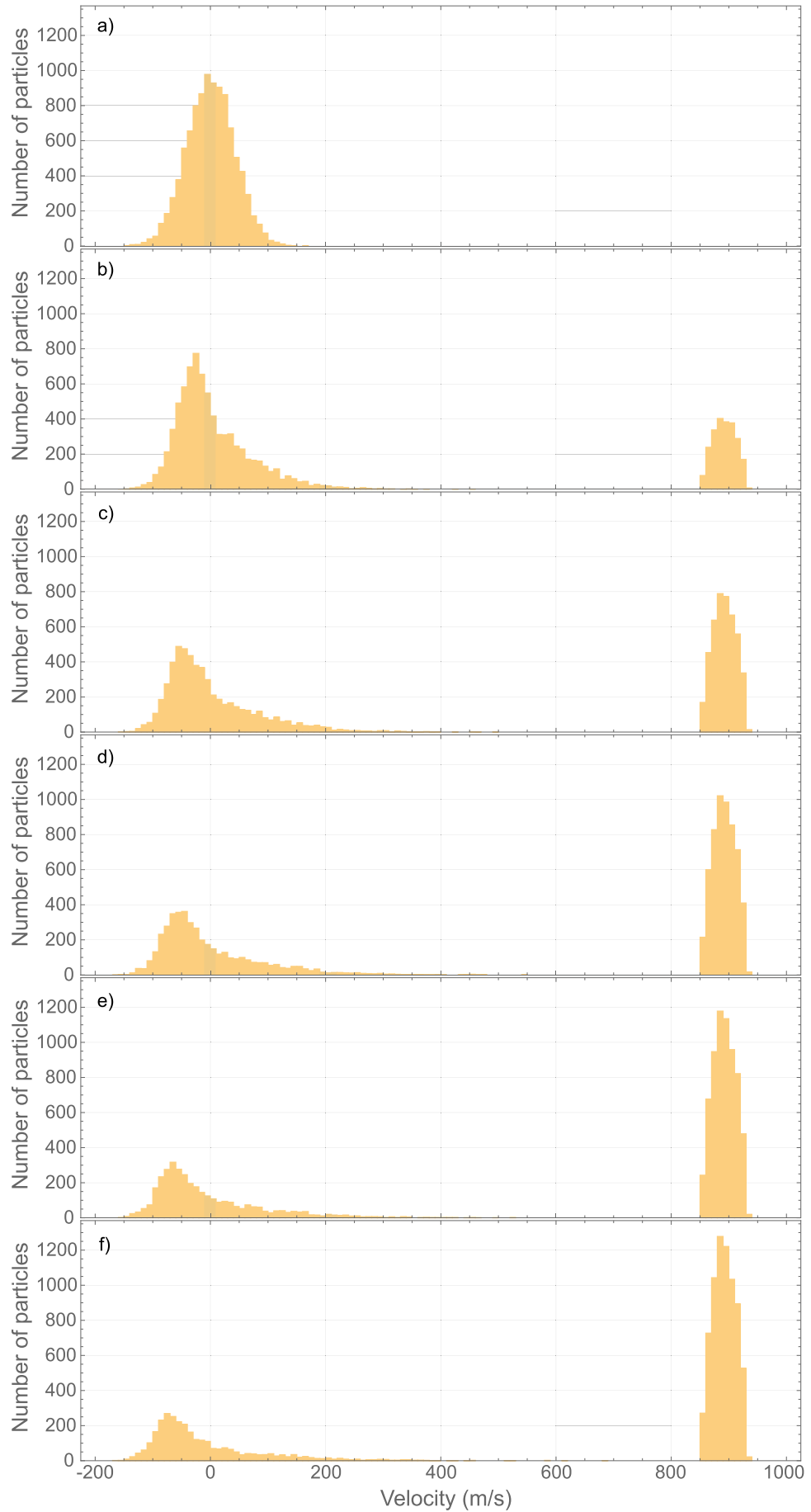


Figure 2. Simulation of acceleration of a 200 mK Maxwell–Boltzmann distribution of 10^4 $\bar{\text{H}}$ atoms using optical lattice parameters described in text. Panel (a) shows initial distribution with zero mean velocity, whilst panels (b)–(f) present, on the left, the remnant unaccelerated sample and right the summed anti-atoms after 1, 3, 5, 7 and 9 laser pulses of 100 ns duration.

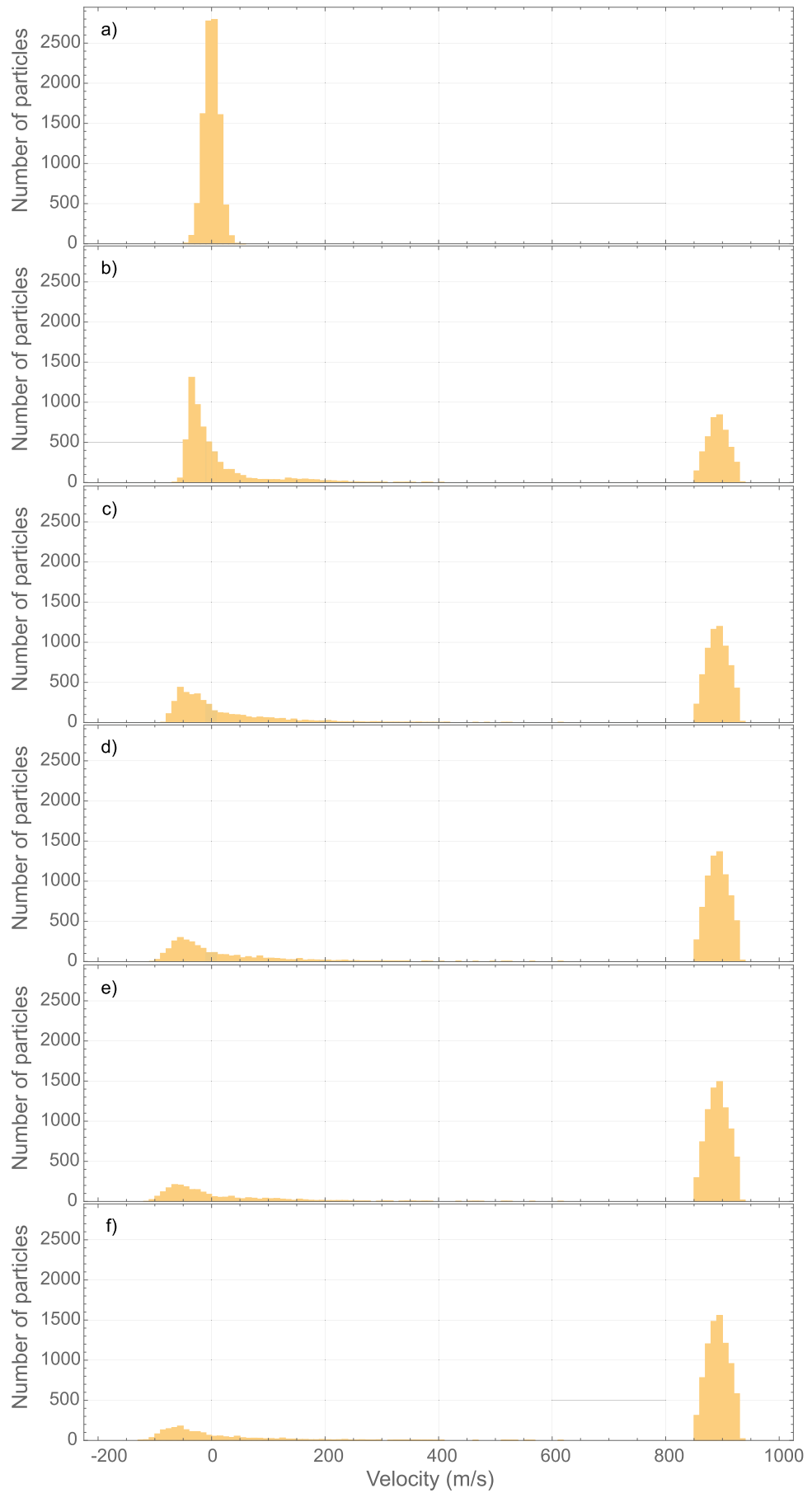
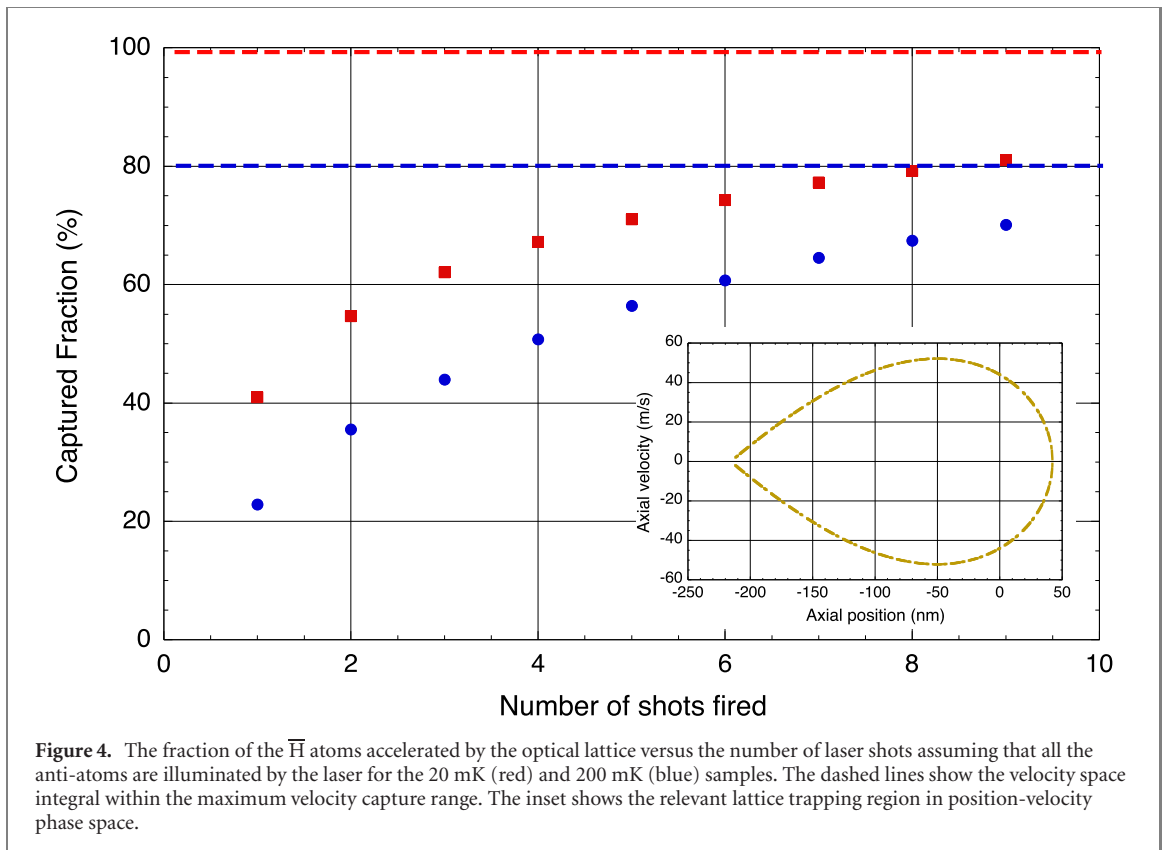


Figure 3. As figure 2 but for an initial \bar{H} sample at 20 mK.



lattice, the condition that

$$\left| \frac{2\beta}{aq} \right| < 1 \quad (5)$$

must be satisfied [49], such that the chirp rate, β , must be

$$\beta < \frac{aq}{2} = \left(\frac{\alpha}{m} \right) \frac{q^2 I_0}{2\epsilon_0 c}, \quad (6)$$

which essentially means that the acceleration of the lattice $a_L = 2\beta/q$ must be less than a , the maximum acceleration supplied by the gradient of the lattice potential [49].

The velocity of the lattice potential due to the chirp is also the average velocity of the particles trapped and is given by

$$v_L = 2\frac{\beta}{q}t < \left(\frac{\alpha}{m} \right) \frac{qI_0 t}{\epsilon_0 c}. \quad (7)$$

Thus, we are able to define a 1D lattice speed v_L by a combination of the laser chirp rate and the pulse duration, and we explore what this capability may provide if applied to an ensemble of trapped $\bar{\text{H}}$ atoms in the following section.

3. Application to trapped antihydrogen

The inner section of the ALPHA apparatus is illustrated schematically in figure 1. This shows the antiparticle trapping and manipulation regions, and in the centre the anti-atom trap. Antihydrogen is fabricated inside the trap, and typically 5×10^4 $\bar{\text{H}}$ atoms are produced by mixing 9×10^4 antiprotons with a cloud of 3×10^6 positrons at a temperature of around 15–20 K. Around 20 of the $\bar{\text{H}}$ s are subsequently held in the 0.54 K deep magnetic minimum atom trap (formed by the octupolar coil and the five mirror coils depicted in figure 1) in a production/trapping cycle that takes around 4 min. This procedure can be repeated, and as mentioned above around a thousand anti-atoms have been accumulated in the trap over a period of about 4 h. The $\bar{\text{H}}$ trap volume is limited radially by the 44.35 mm diameter of the Penning trap electrodes used to confine the charged particles, and axially to a length of about 280 mm by the field from the mirror coils. Studies have shown [4] that the energy distribution of the trapped atoms matches that of a Maxwell–Boltzmann distribution consistent with the positron cloud temperature, but truncated at the 0.54 K depth of the neutral trap.

Very recently ALPHA has succeeded in using the Lyman- α transition to laser-cool a sample of trapped anti-atoms [15]. In these first experiments only one of the $\overline{\text{H}}$ hyperfine states was cooled, with the other ejected (by resonant microwave transfer to an untrapped state) prior to the start of cooling, leaving only 50% of the sample. This was then efficiently cooled by around an order of magnitude in energy to about 20 mK, as suggested by a previous theoretical study [59]. The timescale for the combined anti-atom trapping and cooling procedures, which can be done sequentially or partly in tandem, is around 10 h in total. Note that the final result is an $\overline{\text{H}}$ ensemble in a single (ground) hyperfine state, in particular the low-field seeking $1S_d$ state [15].

In our analysis we assume that $\overline{\text{H}}$ beam production can be effected either before or after laser cooling, with the appropriate starting conditions for the trapped anti-atoms. We also adopt the current laser access conditions to the ALPHA trap, but also point out the possibility, as illustrated schematically in figure 1, of using fully counter-propagating beams to create the optical lattice.

As an example, we take a laser with a wavelength of 1064 nm, a pulse of 100 ns duration and energy 1 J, with a Gaussian beam waist of 200 μm and a chirp of $5.3 \times 10^{16} \text{ rad s}^{-2}$ (or equivalently 8.4 GHz μs^{-1}). The intensity averages to $8 \times 10^{13} \text{ Wm}^{-2}$ within the beam waist, resulting in a maximum acceleration close to $1.6 \times 10^{10} \text{ ms}^{-2}$ using the hydrogen value for α/m of $4.5 \times 10^{-14} \text{ Cm}^2 \text{ V}^{-1} \text{ kg}^{-1}$. Taking the limiting value from equation (7) we find $v_L = 900 \text{ ms}^{-1}$. Using 200 mK (20 mK) as the mean temperature of the trapped $\overline{\text{H}}$ in the ALPHA experiment (see above), we can estimate a transverse speed of the anti-atom of 41 (13) ms^{-1} : thus, the flux may be collimated to within an angle of around 45 (14) mrad.

The time taken for the $\overline{\text{H}}$ to cross the laser beams is typically in excess of 10 μs , so with the laser pulse duration of 100 ns, we expect that most of the anti-atoms captured into the lattice will experience acceleration from the full pulse. If we assume that the $\overline{\text{H}}$ atoms occupy the ALPHA trap uniformly at a density of $n_{\overline{\text{H}}}$, then the number available for acceleration can be estimated as $N_{\text{acc}} = f_L n_{\overline{\text{H}}} V_{\text{ov}}$, with V_{ov} the overlap volume of the lasers beams and f_L the fraction of the overlapped atoms captured by the lattice. In terms of the number of trapped anti-atoms, $N_{\overline{\text{H}}}$, $N_{\text{acc}} = f_L N_{\overline{\text{H}}} V_{\text{ov}} / V_{\text{trap}}$, with V_{trap} the atom trap volume.

In the ALPHA trapping scenario the anti-atoms occupy the entire trap volume of $V_{\text{trap}} \approx 4.2 \times 10^5 \text{ mm}^3$, and with the apparatus currently allowing the laser beams to overlap in the centre of the device at an angle of 2.3° , $V_{\text{ov}} \approx 1.25 \text{ mm}^3$. Assuming $f_L = 0.3$ per laser pulse (see below) we find $N_{\text{acc}} \approx 9 \times 10^{-7} N_{\overline{\text{H}}}$. With the current capabilities of roughly 10^3 trapped anti-atoms $N_{\text{acc}} \approx 10^{-3}$, and for a 1 kHz laser pulse repetition rate fluxes in the region of 1 $\overline{\text{H}}$ atom per second seem feasible. Thus, the trap can be emptied of anti-atoms over a period of 20 min or so whereupon it can then be refilled, and the beam formation cycle repeated as required. Note also that the beam will be timed via the laser pulses, with typical flight times being around milliseconds in duration.

For the cooled, single-(ground)state sample the reduction in transverse speeds will (as mentioned previously) enhance the collimation of the $\overline{\text{H}}$ flux. Furthermore, the cold sample is confined by a field of 60 mT and thus occupies a reduced volume with $V_{\text{trap}} \approx 8 \times 10^4 \text{ mm}^3$, leading to a corresponding increase in the efficiency of beam production by a factor of about five. The superior qualities of the $\overline{\text{H}}$ beam from the cooled sample have to be offset somewhat by the roughly doubling in time needed to achieve the starting conditions for ejection. However, if we consider the case of fully overlapping laser beams applied along the 130 mm length of the trap for the cooled anti-atom sample, beam intensities of several 10s of $\overline{\text{H}}$ per second can be envisaged. It is notable that this geometry will introduce a timing spread into the beam and increase its effective area onto a fixed position target (such as an aperture or detector), when compared to the small-angle overlap geometry described above.

Numerical simulations of the acceleration of the $\overline{\text{H}}$ in the lattice using laser beams with the properties described above have also been performed. The method consists of solving equation (2) using an implicit backward differentiation formula for 10^4 non-interacting particles initially distributed evenly along the axis of the ALPHA trap with a one-dimensional Maxwell–Boltzmann velocity distribution. We have used two distributions with temperatures of 200 and 20 mK. In the experiments antihydrogen is formed at 10s of Kelvin, but the trapped fraction is truncated by the depth of the trap, at around 0.5 K. This truncated distribution is well described by a 200 mK Maxwell–Boltzmann [4]. According to [59], laser-cooling should produce trapped antihydrogen with a temperature reduced to about 20 mK, although it is not expected to result in a thermal distribution. Our treatment of equation (2) ignores motion transverse to the laser (and apparatus) axis as well as variations in laser-power across the beam. The former is justified as transverse motion of the particles is limited to a small fraction of the laser waist for the duration of the pulse.

The simulated speed distributions are shown in figures 2 and 3 for the 200 and 20 mK Maxwell–Boltzmann samples respectively. In both cases the modelled beam has a mean final speed in the z -direction close to the expected value of 900 ms^{-1} . The accelerated sample is shown in these figures for odd numbers of laser pulses (from 1–9), whilst figure 4 shows the fraction of the initial distribution in the beam as the number of laser pulses increases. Note that the simulations assume that all anti-atoms overlap the

lasers, so do not include the effect of the overlap factor, $V_{\text{ov}}/V_{\text{trap}}$, as described above. These studies do show that the fraction captured by the lattice (effectively f_L as defined previously) is in excess of 65% (80%) for 200 (20) mK after a few laser pulses. This is in line with the fraction expected if the dominant effect of repeated pulses is that the lattice eventually captures all particles that have velocities within the limits of the capture phase space of the lattice (given as the inset in figure 4), or said another way, that the constant redistribution of particles in the trap means that most particles with initial velocities within the maximum range of lattice-trappable velocities are captured. We recall that the velocity spread (given by $\sigma = \sqrt{k_B T/m_{\bar{H}}}$) is 12.8 ms^{-1} and 40.6 ms^{-1} for 20 mK and 200 mK respectively and, as shown in figure 4, the maximum particle speed that may be captured is $\sim 52 \text{ ms}^{-1}$.

4. Discussion and concluding remarks

In section 1 we briefly introduced the ASACUSA \bar{H} effort aimed at an investigation of ground state hyperfine structure. For a total anti-atom flight length of somewhat under 2 m, the collaboration has estimated that around 8000 \bar{H} s at a maximum speed of 10^3 ms^{-1} are required to effect the experiment to the desired precision. At the current rate of around 0.4 \bar{H} s on target for a 15 min run cycle, around 200 full days of \bar{p} beam time will be required. Using simple considerations of the estimates given from the current work in section 3, this can be cut substantially (to 10 days or less) using the beam production method proposed herein.

The AEgIS experiment plans to form an \bar{H} beam using the Stark acceleration of Rydberg anti-atoms, and have recently observed [19] the latter formed via the reaction $\bar{p} + \text{Ps}^* \rightarrow \bar{H} + e^-$, with the excited Ps in a state characterised by a principal quantum number, $n = 17$. This will produce \bar{H} in around $n = 24$ [21], though in the high fields present in the experiment there will be a mixture of angular momentum (l) states [60]. Since the AEgIS \bar{H} production is pulsed as a result of the laser excitation of the Ps, it may be feasible to form a Rydberg anti-atom beam using the method discussed herein for their proposed moiré interferometer gravity experiment [61, 62]. According to equation (4) the acceleration is proportional to the product αI_0 and since the polarisability for hydrogen is given (in atomic units) by $\alpha = \frac{n^4}{4} [4n^2 + 14 + 7l(l+1)]$ [63], lattice velocities and capture fractions similar to those for the ground state can be achieved. For instance, there are obvious implications for intensity scaling if the higher lying angular momentum states are considered, where $l \approx n$ such that $\alpha \propto n^6$.

Aside from these investigations, an anti-atom beam such as the one proposed here may find application in the study of cold matter–antimatter interactions and open up the possibility for trap-to-trap transfer. Furthermore, if it is possible to laser stimulate the production of low-lying \bar{H} states, either directly from the continuum (see e.g., [64, 65]) or from highly excited states [66], the production of beams of the metastable 2S state may be foreseen. For this state α is around $27\times$ that for the ground state, which will result in a proportionate reduction in laser intensity to mitigate the possibility of multi-photon ionization.

We believe that the proposed method of \bar{H} beam formation via the acceleration of trapped anti-atoms using a travelling optical lattice has advantages over reliance on the directional properties of \bar{H} produced via reaction 1. The \bar{H} speed can be varied by altering v_L via the chirp rate and/or the pulse duration, and the latter means that the beam is timed to aid in event isolation and background suppression. The trapped atoms are all in their ground state prior to acceleration, and with a phase space distribution that is understood [4] and reproducible.

Our method should provide fluxes that are scalable with the new ELENA facility, which will produce lower energy \bar{p} beams at the AD [67, 68] and enhance \bar{H} production and trapping capabilities by one or two orders of magnitude. Ongoing efforts (e.g., [69–71]) to lower the temperature of the positron plasma will yield increases in ALPHA's \bar{H} trapping rates [72], leading to further possible enhancements in beam flux. In future it may be possible to hold in excess of 10^5 laser-cooled, ground state, \bar{H} atoms in readiness for extraction in a beam using the method described herein.

Acknowledgements

We thank the EPSRC (UK) for support of our antihydrogen work. We are grateful to Professor Peter Barker for useful discussions and for help in the early stages of the work.

Data availability statement

All data that support the findings of this study are included within the article (and any supplementary files).

ORCID iDs

N Madsen  <https://orcid.org/0000-0002-7372-0784>

M Charlton  <https://orcid.org/0000-0002-9754-1932>

References

- [1] Andresen G B *et al* (ALPHA Collaboration) 2010 *Nature* **468** 673
- [2] Andresen G B *et al* (ALPHA Collaboration) 2011 *Phys. Lett. B* **695** 95
- [3] Gabrielse G *et al* (ATRAP Collaboration) 2012 *Phys. Rev. Lett.* **108** 113002
- [4] Andresen G B *et al* (ALPHA Collaboration) 2011 *Nat. Phys.* **7** 558
- [5] Ahmadi M *et al* (ALPHA Collaboration) 2017 *Nat. Commun.* **8** 681
- [6] Amole C *et al* (ALPHA Collaboration) 2013 *Nat. Commun.* **4** 1785
- [7] Amole C *et al* (ALPHA Collaboration) 2014 *Nat. Commun.* **5** 3955
- [8] Ahmadi M *et al* (ALPHA Collaboration) 2016 *Nature* **530** 373
- [9] Amole C *et al* (ALPHA Collaboration) 2012 *Nature* **481** 439
- [10] Ahmadi M *et al* (ALPHA Collaboration) 2017 *Nature* **541** 506
- [11] Ahmadi M *et al* (ALPHA Collaboration) 2020 *Nature* **578** 375
- [12] Ahmadi M *et al* (ALPHA Collaboration) 2017 *Nature* **548** 66
- [13] Ahmadi M *et al* (ALPHA Collaboration) 2018 *Nature* **557** 71
- [14] Ahmadi M *et al* (ALPHA Collaboration) 2018 *Nature* **561** 211
- [15] Baker C J *et al* (ALPHA Collaboration) 2021 *Nature* **592** 35
- [16] Enomoto Y *et al* 2010 *Phys. Rev. Lett.* **105** 243401
- [17] Kuroda N *et al* 2014 *Nat. Commun.* **5** 3089
- [18] Krasnický D *et al* (AEGIS Collaboration) 2014 *Int. J. Mod. Phys.* **30** 1460262
- [19] Amsler C *et al* (AEGIS Collaboration) 2021 *Commun. Phys.* **4** 19
- [20] van der Werf D P 2014 *Int. J. Mod. Phys. Conf. Ser.* **30** 1460263
- [21] Charlton M 1990 *Phys. Lett. A* **143** 143
- [22] Kadyrov A S, Bray I, Charlton M and Fabrikant I I 2017 *Nat. Commun.* **8** 1544
- [23] Amoretti M *et al* (ATHENA Collaboration) 2002 *Nature* **419** 456
- [24] Gabrielse G *et al* (ATRAP Collaboration) 2002 *Phys. Rev. Lett.* **89** 213401
- [25] Holzschteier M H, Charlton M and Nieto M M 2004 *Phys. Rep.* **402** 1
- [26] Amoretti M *et al* (ATHENA Collaboration) 2004 *Phys. Lett. B* **590** 133
- [27] Gabrielse G 2005 *Adv. At. Mol. Opt. Phys.* **50** 155
- [28] Robicheaux F 2004 *Phys. Rev. A* **70** 022510
- [29] Robicheaux F 2008 *J. Phys. B: At. Mol. Opt. Phys.* **41** 192001
- [30] Jonsell S, van der Werf D P, Charlton M and Robicheaux F 2009 *J. Phys. B: At. Mol. Opt. Phys.* **42** 215002
- [31] Jonsell S, Charlton M and van der Werf D P 2016 *J. Phys. B: At. Mol. Opt. Phys.* **49** 134004
- [32] Jonsell S and Charlton M 2021 *J. Phys. B: At. Mol. Opt. Phys.* **54** 025001
- [33] Madsen N *et al* (ATHENA Collaboration) 2005 *Phys. Rev. Lett.* **94** 033403
- [34] Jonsell S and Charlton M 2019 *New J. Phys.* **21** 073020
- [35] Gabrielse G, Fei X, Orozco L A, Tjoelker R L, Haas J, Kalinowsky H, Trainor T A and Kells W 1989 *Phys. Rev. Lett.* **63** 1360
- [36] Eriksson T 2009 *Hyperfine Interact.* **194** 123
- [37] Zhmoginov A I, Charman A E, Shaloo R, Fajans J and Wurtele J S 2013 *Class. Quantum Grav.* **30** 205014
- [38] Nagata Y *et al* 2017 *JPS Conf. Proc.* **18** 011007
- [39] Kolbinger B *et al* ASACUSA Collaboration 2018 *EPJ Web Conf.* **181** 01003
- [40] Malbrunot C *et al* 2018 *Phil. Trans. R. Soc. A* **376** 20170273
- [41] Kolbinger B *et al* 2021 *Eur. Phys. J. D* **75** 91
- [42] Widmann E *et al* 2003 *Letter of Intent CERN/SPSC 2003-009 SPSC-I-226* <http://dx.doi.org/10.17181/CERN.09QI.13NK>
- [43] Diermaier M *et al* 2017 *Nat. Commun.* **8** 15749
- [44] Radics B, Murtagh D J, Yamazaki Y and Robicheaux F 2014 *Phys. Rev. A* **90** 032704
- [45] Radics B and Yamazaki Y 2016 *J. Phys. B: At. Mol. Opt. Phys.* **49** 064007
- [46] Lundmark R, Malbrunot C, Nagata Y, Radics B, Sauerzopf C and Widmann E 2015 *J. Phys. B: At. Mol. Opt. Phys.* **48** 184001
- [47] Widmann E *et al* 2019 *Hyperfine Interact.* **240** 5
- [48] Kolbinger B, Capon A, Diermaier M, Lehner S, Malbrunot C, Massiczek O, Sauerzopf C, Simon M C and Widmann E 2015 *Hyperfine Interact.* **233** 47
- [49] Barker P F and Shneider M N 2001 *Phys. Rev. A* **64** 033408
- [50] Maher-McWilliams C, Douglas P and Barker P F 2012 *Nat. Photon.* **6** 386
- [51] Fulton R, Bishop A I, Shneider M N and Barker P F 2006 *Nat. Phys.* **2** 465
- [52] Bishop A I, Wang L and Barker P F 2010 *New J. Phys.* **12** 073208
- [53] Barker P F and Charlton M 2012 *New J. Phys.* **14** 045005
- [54] Takakoshi T and Knize R J 1996 *Opt. Lett.* **21** 77
- [55] Dörr M, Potvliege R M and Shakeshaft R 1990 *J. Opt. Soc. Am. B* **7** 433
- [56] Lambropoulos P and Tang X 1987 *J. Opt. Soc. Am. B* **4** 821
- [57] Barker P F and Shneider M N 2001 *Phys. Rev. A* **66** 065402
- [58] Dong G, Lu W and Barker P F 2003 *J. Chem. Phys.* **118** 1729
- [59] Donnan P H, Fujiwara M C and Robicheaux F 2013 *J. Phys. B: At. Mol. Opt. Phys.* **46** 025302
- [60] Antonello M *et al* (AEGIS Collaboration) 2020 *Phys. Rev. A* **102** 013101
- [61] Doser M *et al* (AEGIS Collaboration) 2012 *Class. Quantum Grav.* **29** 184009
- [62] Aghion S *et al* (AEGIS Collaboration) 2014 *Nat. Commun.* **5** 4538
- [63] Baye D 2012 *Phys. Rev. A* **86** 062514
- [64] Wolf A 1993 *Hyperfine Interact.* **109** 233

- [65] Müller A and Wolf A 1997 *Hyperfine Interact.* **76** 189
- [66] Wolz T, Malbrunot C, Vielle-Grosjean M and Comparat D 2020 *Phys. Rev. A* **101** 043412
- [67] Maury S *et al* 2014 *Hyperfine Interact.* **229** 105
- [68] Bartmann W *et al* 2018 *Phil. Trans. R. Soc. A* **376** 20170266 on behalf of the ELENA and AD teams
- [69] Madsen N, Robicheaux F and Jonsell S 2014 *New J. Phys.* **16** 063046
- [70] Sameed M, Maxwell D and Madsen N 2020 *New J. Phys.* **22** 013009
- [71] Jones J, Madsen N, Maxwell D T and Peszka J ALPHA Collaboration 2021 in preparation
- [72] Jonsell S and Charlton M 2018 *New J. Phys.* **20** 043049